

## Article

# The Design of a Process for Adsorbing and Eluting Chromium (VI) Using Fixed-Bed Columns of *E. crassipes* with Sodium Tripolyphosphate (TPP)

Uriel Fernando Carreño Sayago \* and Vladimir Alfonso Ballesteros Ballesteros

Facultad de Ingenieria, Fundacion Universitaria los Libertadores, 111221 Bogotá, Colombia

\* Correspondence: ufcarrenos@libertadores.edu.co

**Abstract:** Proper water resource management is a critical global objective, both privately and in business, due to the continuous deterioration of this valuable resource. Scientific research in environmental sciences has made significant progress in the development and achievements of treatment. The use of transformed *E. crassipes* biomass with sodium tripolyphosphate (TPP) can help to achieve this important goal. The objective of this study was to develop an experimental process for the continuous adsorption and elution of chromium (VI) using fixed-bed columns of *E. crassipes* biomass modified with sodium tripolyphosphate (TPP). Additionally, design tools were created, and economic viability was assessed by analyzing adsorption capacity indicators and unit production costs of different biomasses. Treatment systems were designed and constructed to remove chromium from tannery wastewater, ensuring that the levels were below the current environmental regulations of 0.05 mg/L Cr(VI). The biomass had an adsorption capacity of 98 mg/g and was produced at a low cost of 8.5 dollars. This resulted in an indicator of 11.5 g Cr(VI)/(USD) when combined with the elution processes. The proposed strategy, which utilizes entirely green technologies, enables the recovery and valorization of water resources. This makes it an effective tool for the circular economy.

**Keywords:** *E. crassipes*; treatment water; tripolyphosphate (TPP); chromium



**Citation:** Sayago, U.F.C.; Ballesteros, V.A.B. The Design of a Process for Adsorbing and Eluting Chromium (VI) Using Fixed-Bed Columns of *E. crassipes* with Sodium Tripolyphosphate (TPP). *Water* **2024**, *16*, 952. <https://doi.org/10.3390/w16070952>

Academic Editors: Issam A. Al-Khatib, Rehab O. Abdel Rahman, Tsuyoshi Imai and Yung-Tse Hung

Received: 12 February 2024

Revised: 13 March 2024

Accepted: 14 March 2024

Published: 26 March 2024



**Copyright:** © 2024 by the authors. Licensee MDPI, Basel, Switzerland. This article is an open access article distributed under the terms and conditions of the Creative Commons Attribution (CC BY) license (<https://creativecommons.org/licenses/by/4.0/>).

## 1. Introduction

Non-conventional, economical, and efficient treatment is a major focus of research centers in developing countries, where wastewater from rivers, wetlands, and other water sources is still contaminated with heavy metals, phenols, and dyes. For this reason, there is a need to find suitable ways to treat water in an efficient way in the industrial sector, where most of the pollution occurs. One suitable method of treating industrial wastewater is through fixed-bed column systems, coupled with a process of reutilizing waste biomasses [1–3].

Fixed-bed columns are those with a constant biomass, together with pollutant flow inputs, which are easy to implement, effective due to the chelating capacity of the biomass, and economical. In different research, such as [4–6], treatment systems have been designed for large water bodies due to their mass balance models and intra-particle and ex-particle diffusion among other models and isotherms [7,8].

Among the varieties of heavy metal, the most impactful on water resources is chromium, which is utilized across a variety of industries due to its efficacy in metal alloys and the tannery industry's leather preservation techniques. However, its excessive use has resulted in significant environmental, social, and health issues [9]. A notable instance of this environmental threat can be observed in the south of Bogotá, Colombia. Over 350 tanneries in this area utilize chromium (VI), which is discharged into the Tunjuelo River and deteriorates its quality, thereby diminishing the ecosystem services available to the communities adjacent to the river [10].

To carry out sustainable projects, various plant species' biomasses have been used due to their high elimination efficiency, natural availability, and profitability, which favor

the chemisorption process [11–13]. Chemisorption is a widely used technique for treating industrial wastewater due to its low cost and ability to remove various contaminants, as well as the ease of regenerating the adsorbent [14–16].

The presence of hydroxyl (OH) and carboxylic (COOH) groups in cellulose leads to the removal of heavy metals by adsorption through cation exchange or chemical mechanisms [17,18]. This cellulose is found in considerable amounts within the aquatic plant *E. crassipes* [19–22], which is abundant in tropical environments due to its dry biomass resulting from regular cleaning in the wetlands, lagoons, and rivers of Bogotá D.C. [23,24].

Pilot-scale process trials offer assistance in designing treatment systems that meet discharge regulations [25–28]. To create greater consistency in biomass and improve the heavy metal chemisorption process, the adsorption of heavy metals on modified cellulose involving sodium tripolyphosphate (TPP) has been investigated [29–31]. Microspheres, comprising *E. crassipes* and sodium tripolyphosphate (TPP), were examined for their ability to adsorb lead (II). This novel adsorbent exhibited a maximum loading capacity of 312.5 mg/g [32].

This current study selected adsorption with the chelating biomass of *E. crassipes* as the method for removing chromium (VI) from industrial wastewater at a tannery south of Bogota. The primary novelty of this research lies in the use of mathematical models in the adsorption and elution phases of fixed-bed processes. This study aims to create an experimental process for adsorbing and eluting chromium (VI), using fixed-bed columns of *E. crassipes* biomass modified with sodium tripolyphosphate (TPP), and operate it continuously. This study also seeks to develop design tools and determine economic viability by analyzing the adsorption capacity indicators and unit production costs of different biomasses.

## 2. Materials and Methods

**Aquatic plants:** The roots and leaves of the aquatic plant *E. crassipes* were taken from the Juan Amarillo wetland in the city of Bogotá D.C. The aim was to obtain particle diameters of 0.212 mm (it should be less than 0.212 mm for better contact between particle and contaminate [1,2]).

**Chromium measurement:** The samples were analyzed in a flask at each time interval, evaluated for the residual chromium of 20 µm samples, and subsequently centrifuged (KASAI MIKRO 200). Residual chromium was measured using a UV84.

**Determination of chromium:** This was conducted via the diphenylcarbazide method, which involved preparing a phosphate-buffer solution and adjusting it to a pH equal to 2; the degree of purity was 90% (H<sub>3</sub>PO<sub>4</sub>). Subsequently, 200 µL of 0.5% diphenylcarbazide was added to an Eppendorf tube, with its purity being 97%, together with acetone *w/v*; it also had a purity of 97%. An amount of 900 µL of phosphate buffer and 100 µL of the residual sample were obtained, and these were finally taken to an absorption cell, with the absorbance measuring 540 nm. On an Evolution 300 spectrophotometer, changes in absorbance were monitored. All evaluations were performed under the APHA (American Public Health Association Procedure) for standard tests (standard methods for the examination of water and wastewater). All experiments were carried out in triplicate, with final values averaged.

**Fixed biomass column experiments:** Treatment systems were developed in recycled plastic containers, coupled with interconnection processes between biocapsules (each capsule had 30 g of dry biomass, along with the reagent). The height was 40 cm, and the diameter was 4.5 cm, with an area of 30 cm<sup>2</sup> established and for a total of 1000 cm<sup>3</sup> in volume. The flow rate was 20 mL/min, kept constant by constant flow through the drip.

**Preparation of *E. crassipes* beads.** Approximately 100 g of *E. crassipes* powder was dissolved in 150 mL of diluted acetic acid (2% (*v/v*)), and then this solution was gently stirred and mixed with 250 mL and 500 mL of sodium tripolyphosphate (TPP) Na<sub>5</sub>O<sub>10</sub>P<sub>3</sub>, molecular weight 367.86, solution at pH 8.6 to form the gelled spheres. This procedure had

to be repeated five times to obtain sufficient material [32]. Two types of experiments were carried out:

Two similar treatment systems were built, changing only the way they will be distributed in the treatment system.

*E. crassipes* with 250 mL (TPP) mixed with 100 g EC biomass EC + TPP (1)

*E. crassipes* with 500 mL (TPP) mixed with 100 g EC biomass EC + TPP (2)

The system is shown in Figure 1.

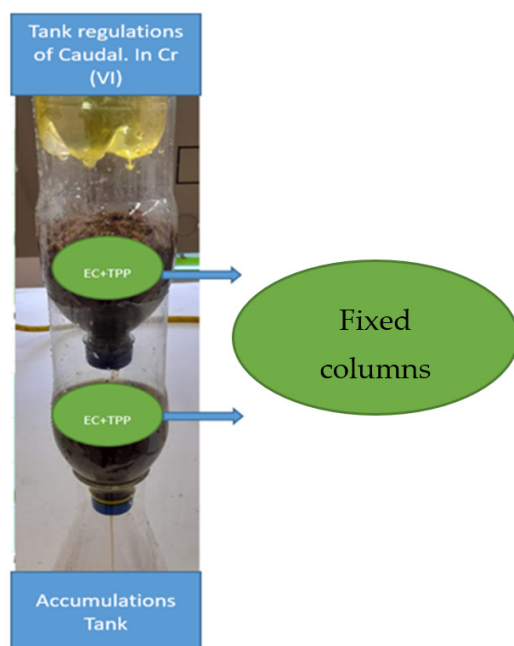


**Figure 1.** Design of treatment with EC+TPP.

Evaluating initial concentrations of 1000 mg/L of Cr(VI). All the tests were carried out in duplicate, calculating the average between the data obtained and with this the percentage of metal removal.

Adsorption models. Mathematical modelling was used to describe the behavior of the rupture curves, aiding in comprehension and scaling of the system. The biosorption process of Cr(VI) in the fixed-bed configuration was explained by fitting the breakthrough curve data to three different column adsorption models: Yoon-Nelson, Thomas, and Bohart.

The study used the widely accepted Thomas model to estimate the maximum adsorption capacity and predict the rupture curves. The proposed model assumed a second-order kinetic of reversible reactions and the Langmuir isotherm [33]. Additionally, the Thomas model was used to validate the proposed model, demonstrating its effectiveness.

The Yoon-Nelson model assumes that the rate of adsorption decreases proportionally to the curve of adsorbate removal and adsorbent breakdown, without considering factors such as adsorbate properties, adsorbent type, and adsorption column specifications [34].

However, the Bohart equation is commonly used to quantify various types of systems due to its ability to describe the relationship between  $C/C_0$  and  $t$  in a continuous system with clarity and confidence. The model states that the rate of sorption is directly proportional to the remaining capacity of the solid and the concentration of the retained species. This model is specifically used to describe the initial part of the rupture curve. Table 1 presents the various adsorption models [35].

**Table 1.** Adsorption models.

Thomas model	(1)	$\ln \frac{C_0}{C} - 1 = \frac{K_{th} \times q \times m}{Q} - K_{th} \times C_0 \times T_b$
Yoon model	(2)	$\frac{C}{C_0} = \frac{1}{1 + \exp(K_{YN}(y - t))} qN = \frac{T_b C_0 Q}{m}$
Bohart model	(3)	$T_b = \frac{N_0}{C_0 U} Z - 1 \ln \frac{1}{K_b C_0} \ln \left( \frac{C_0}{C} - 1 \right)$
Model Carreño	(4)	$q = \frac{Q T_b C_0}{M} - \frac{Q T_b C_f}{M} - \frac{\epsilon V C_0}{M}$

The Model Carreño contains all the necessary parameters for designing a treatment system, including the relationships between densities, rupture time, and flow. Although this model is not adjusted, it is used to determine the adsorption capacity [36].

Co: initial concentration of Cr(VI); C: final Cr(VI); V: volume; KTh: Thomas constant (mL/mg·min); q: adsorption capacity (mg Cr/g biomass); m: mass of biomass in column (g); Q: flow rate through the column (mL/min); Tb: time of rupture (min); K YN: Yoon and Nelson constant (1/h), q:  $\gamma$  capacity (mg/g), dynamic capacity (mg/dm<sup>-3</sup>); Z: bed height (cm); U: linear flow rate (cm/min); and Kb: Bohart constant (1/h).

Analysis of reliability. Reliability is a useful tool for establishing efficiency and compliance characteristics in environmental processes [37]. The exponential equation reflects the behavior of data in contaminant removal processes [38].

$$P(X \leq X_s) = 1 - \exp\left\{-\frac{x}{\sigma}\right\}, \quad x \geq 0 \quad (5)$$

X = Continuous random variable mg/L;

$\sigma$  = Arithmetic average 0.05 mg/L Cr(VI).

The materials were characterized. This process used a TESCAN FE-MEB LYRA3 scanning electron and focused ion beam microscope. The SEM had an integrated X-ray energy dispersion spectroscopy microanalysis system, EDS (energy dispersive X-ray spectroscopy). EDS is one of the most efficient techniques for the qualitative and quantitative analysis of organic samples and, through the SEM microphotographs, the samples evaluated in the present investigation were observed in detail; the diffraction of an X-ray beam by the atoms of the sample interacts with the X-ray beam, producing regions of diffraction intensity, or peaks, for the diagnosis of each of the elements.

FTIR. The materials were characterized by Fourier transform infrared spectroscopy (79 Jasco FTIR 430) to measure IR spectra in a spectral range of 4000–400 cm<sup>-1</sup>, a resolution of 4 cm<sup>-1</sup>, and a scanning speed of 2 mm s<sup>-1</sup>.

### 3. Results

FTIR spectral details. When comparing the FTIR spectral details of the cellulose with TPP and the same cellulose after the treatment process, it was observed that the EC-TPP-Cr(VI) showed some new bands compared to that of the untreated biomass in Figure 2.

It can be observed that the biomass without the EC-TPP treatment process exhibits a deep peak due to the presence of hydroxyl groups (OH), in comparison with the biomass of the EC alone, which has a lower wavenumber [1]. This suggests that there is an effective interaction between the sodium tripolyphosphate and the cellulose of *E. crassipes*. Additionally, there is a peak (P=O) at 1210 cm<sup>-1</sup> and another peak representing (P-OH) at 1038 cm<sup>-1</sup>; the stretching band is attributed to the presence of phosphorus, while the characteristic band of the amine group in vegetable cellulose at 1650 cm<sup>-1</sup>, similar to (CH) at 1032 cm<sup>-1</sup>, is also observable. A graph comparing the two biomasses before and after the treatment processes is presented to identify potential sites for Cr(VI) ion binding.

After conducting the Cr(VI) adsorption process using EC-TPP biomass, a shift towards a lower wavenumber was observed in the peak at 3424.96 cm<sup>-1</sup> of the (OH) groups, as well as the amine group. This suggests the formation of an interaction between the Cr(VI)

ions and the nitrogen atoms, indicating that nitrogen atoms may be the primary adsorption sites for metal ion binding. Furthermore, the intensity of P-O-H was reduced after the adsorption of Cr(VI) ions.

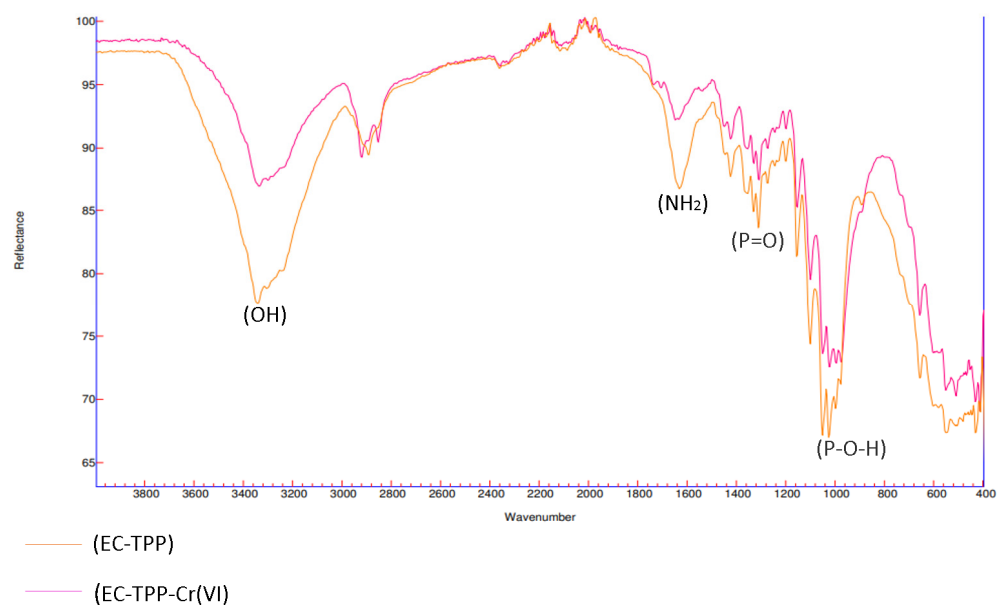


**Figure 2.** Characterizations with FTIR of EC-TPP.

SEM and EDS analysis. Figure 3 displays images of the EC+TPP biomass prior to the adsorption process of Cr(VI) ions. The surface morphology observed in the image indicates an effective articulation between the sodium tripolyphosphate and the cellulose of *E. crassipes*, with a monolayer also being detectable.

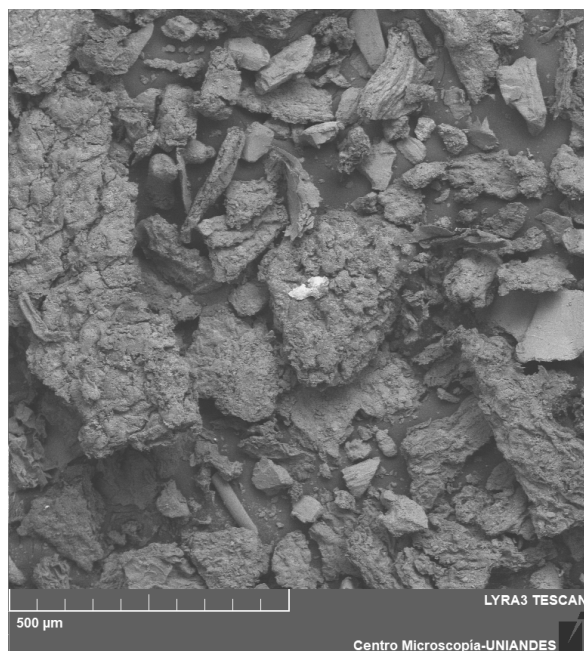


**Figure 3.** Microphotograph of EC+TPP.

The presence of white particles of Cr(VI) ions on the surface confirms the occurrence of the adsorption process. To better observe the images of each characteristic element, they were identified with colors, as shown in Figure 4a–c.

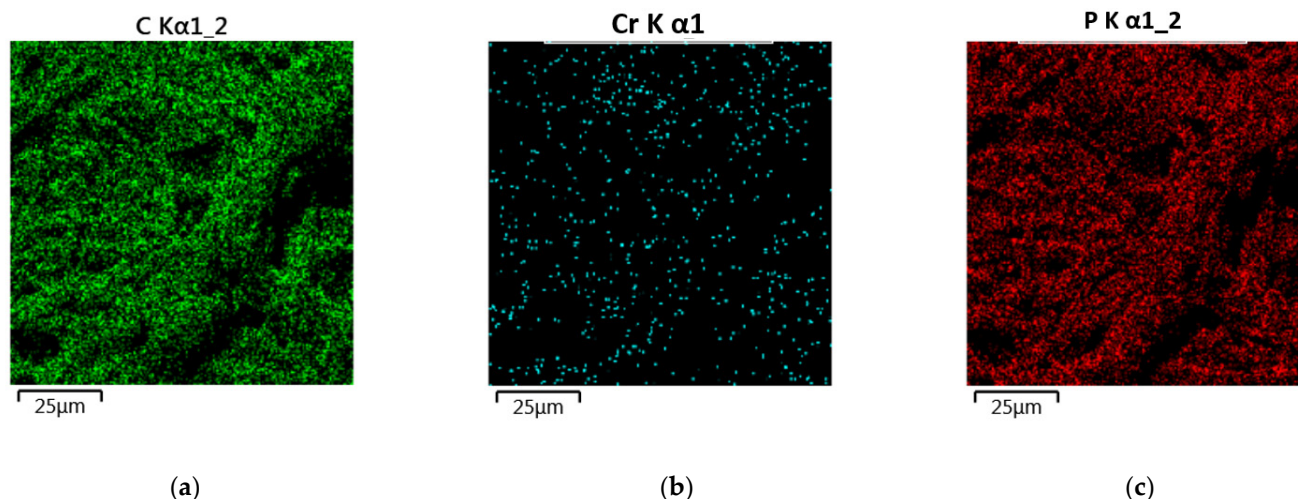


**Figure 4.** Photomicrographs of EC+TPP with Cr(VI). (a) Photograph with the presence of carbon; the presence of Cr(VI) is shown in image (b), and the presence of phosphorous in image (c).

In the microphotograph displayed in Figure 4, the green dots represent carbon (special components of the *E. crassipes* biomass), red dots represent phosphorus (representative of TPP), and the blue represent the Cr(VI), which remains removed from the EC+TPP biomass through cation exchange processes with the hydroxyl groups (OH) present in the EC+TPP biomass. Table 2 shows the physicochemical characterization of the EC+TPP sample by EDS.

**Table 2.** Physicochemical characterization of the EC sample.

Element	Weight	Porcentaje %
Oxygen	48.64	46.67
Carbon	38.15	36.94
Phosphorous	9.13	7.37
Sodium	10.2	9.8

The EDX spectra of the bead suggest that the cross-linking processes between the biomass and the TPP have occurred efficiently, as evidenced by the observations of phosphorus and sodium. The results are summarized in Table 3. Following the Cr(VI) adsorption process, the EDX spectra of the bead were analyzed and the findings are summarized in Table 3.

**Table 3.** Physicochemical characterization of the EC-TPP+Cr sample.

Element	Weight	Percentage %
Oxygen	43.64	41.67
Carbon	35.15	33.94
Phosphorous	9.13	7.37
Sodium	7.3	7.8
Chromium	9.2	8.3

Table 3 shows the characterization of the elements and it can be observed that at 10% by weight, an adhesion of this heavy metal is evident in the samples. Similar results were presented in [29]. A summary of the physicochemical characteristics evidenced in the FTIR samples and SEM microphotographs are shown in Figure 5, where a cellulose sample transformed with TPP adheres to Cr(VI).

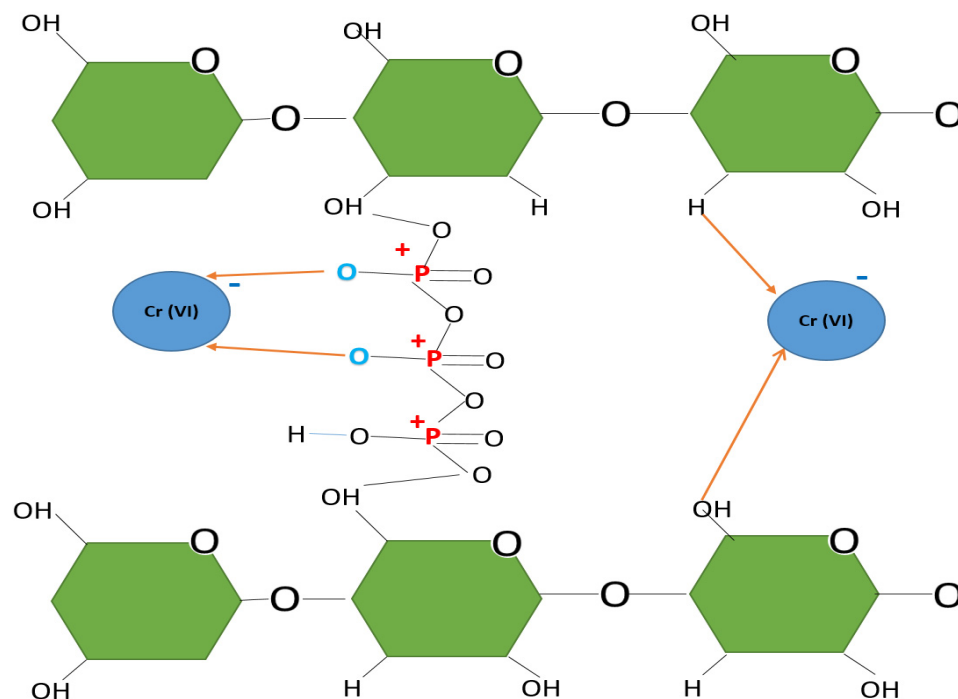
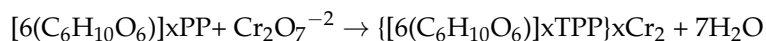


Figure 5. Representations of adsorptions.

Cellulose reacts with TPP to form chelating complexes, increasing the active sites where Cr(VI) will reside. The contact between the  $\text{Cr}_2\text{O}_7$  dichromate and the biomass loaded with active sites generates reactions between the  $(\text{H}^+)$  of the biomass and the oxygen of the Cr(VI) structure, reducing it to Cr(III), which is chromium oxide  $\text{Cr}_2\text{O}_3$ .



According to Figure 5, it can be observed that 6 parts of glucose react with dichromate, where  $([6(\text{C}_6\text{H}_{10}\text{O}_6)]\text{xTPP})$  represents the biomass and  $\text{Cr}_2\text{O}_7^{-2}$  represents Cr(VI). These graphical representations are based on the conclusions drawn from the microphotographs and FTIR analysis.

The results of the process of adsorption of the Cr(VI) column experiments are shown in Figure 6. The configuration of the process used for the removal of Cr(VI) from the actual effluent uses fixed-bed columns in series. The yield is shown with an initial concentration of 1000 mg/L.

The EC+PPT treatment (1) achieved a consistent removal rate of 99% in all cases, as demonstrated in Figure 6a, with a breakpoint occurring at a volume of 4 L. With a flow rate of 20 mL/min, the breaking point is reached after 350 min. In the case of biomass, the EC+PPT treatment (2) resulted in the elimination of 99% of the contaminants after processing approximately 5 L of water. This biomass treated more water and achieved better yields due to its higher PPT content, reaching its breaking point in approximately 420 min. The biomass of *E. crassipes*, without any modification, could treat around 2 L of this same water [1], but with the addition of PPT better yields of up to more than two liters more water could be achieved. The addition of chemical agents to this type of biomass also improved the treatment yields, such is the case of the xanthate biomass of *E. crassipes*, where around 3.5 L of contaminated water was treated under the same concentrations [20]. The addition of PPT achieved better yields due to the expansion of active sites in the EC biomass [29–31].

**Analysis of Reliability.** The permissible limits for Cr(VI) ions in drinking water prescribed by the World Health Organization (WHO) are 0.05 mg/L. The results shown in Table 4 show the final concentration of Cr(VI) mg/L. Table 4 shows the results of the process of removals.

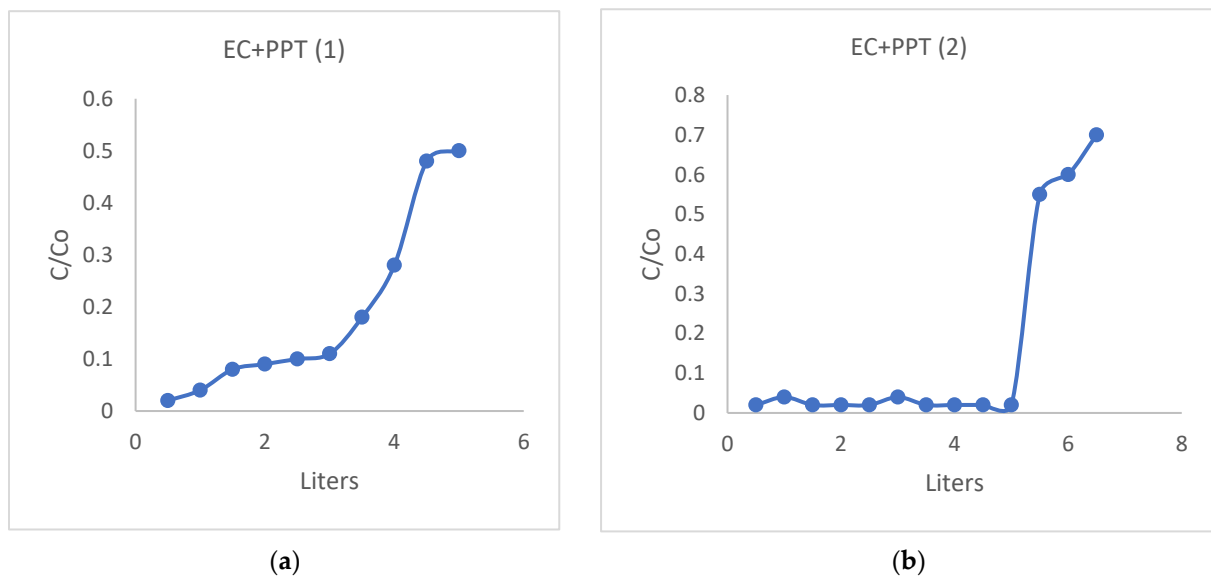


**Figure 6.** Treatment with the biomass EC+PPT. Figure (a) shows the biomass EC+PPT (1), and the biomass EC+PPT (2) is shown in (b).

**Table 4.** Reliability analysis of the results.

	EC-PPT (1)	EC-PPT (2)
Liters	Concentrations End of Cr(VI) (mg/L)	
0.5	0.04	0.02
1	0.04	0.01
1.5	0.05	0.01
2	0.04	0.01
2.5	0.05	0.01
3	0.05	0.01
3.5	0.05	0.02
4		0.02
4.5		0.02
5		0.02
5.5		0.02
Average	0.04	0.02
Standard deviation	0.04	0.004

Kolmogorov–Smirnov tests were carried out to check the distribution of the data while the efficiency tests were carried out; the data behave under an exponential distribution in both biomasses. It is ideal to comply with national and international regulations, with Cr(VI) values below 0.05 mg/L of Cr(VI); through Equation (5), the probability of this value was determined.

$$P(X \leq 0.05) = 1 - \exp\left\{-\frac{0.05}{0.02}\right\},$$

The reliability of the system with the EC-PPT biomass (2) is 80%, which exceeds regulatory values due to its high removal efficiency. Meanwhile, the reliability of the EC-PPT biomass (1) is 61% under an exponential distribution, which meets the standard. The most appropriate biomass is selected based on statistical data stabilization. Experiments must comply with regulations and have suitable probability distributions for both simulations and experiment replications [39,40].

Model of adsorptions. This section uses the Thomas model to validate the Carreño Equation and establish the behavior of the treatment process. The Thomas model estimates the maximum adsorption capacity and predicts the breakthrough curves, assuming re-

versible second-order reaction kinetics and a Langmuir isotherm [41,42]. Tables 5 and 6 present the parameters of the Thomas, Yoon, and Bohart equations.

**Table 5.** Summary of the experimental results obtained with EC-PPT (1).

	EC-PPT	Bohart	Yoon	Thomas
1000 mg/L	K R <sup>2</sup>	0.048 K <sub>b</sub> 0.99	0.039 K <sub>YN</sub> 0.9444	0.055 K <sub>Th</sub> 0.954

**Table 6.** Summary of the experimental results obtained with EC-PPT (2).

	EC-PPT (2)	Bohart	Yoon	Thomas
1000 mg/L	K R <sup>2</sup>	0.061 K <sub>b</sub> 0.90	0.05 K <sub>YN</sub> 0.9444	0.061 K <sub>Th</sub> 0.966

A representative fit of the Thomas equation was observed, although significant adjustments were made to Bohart and Yoon. The Thomas constant was found to be 0.055 mL/mg·min, indicating the chemisorption rate of Cr(VI) into the EC-PPT biomass. The modified biomass has a Cr(VI) adsorption rate of 0.035 mL/mg·min, which is higher than the unmodified biomass but lower than that of the EC-PPT biomass (2), which reached a rate of 0.061 mL/mg·min. The better behavior of the modified biomass in the adsorption of Cr(VI) is evident. Table 6 shows the fitted parameters for EC-PPT biomass (2).

Both the EC-PPT (1) and EC-PPT (2) biomass fit the mathematical Thomas model well, with an R<sup>2</sup> value exceeding 95%. The Langmuir isotherm and second-order kinetics provide evidence of diffusivity in a monolayer for all processes. Equation (4) was validated, and the adsorption capacities were determined for each adsorption and desorption process using the Thomas equation. Table 7 shows a summary of the experimental results obtained.

**Table 7.** Summary of the experimental results obtained.

	Biomass	q (Thomas)	q (Carreño) mg/g
1000 mg/L	EC-PPT (1)	17.9	17
1000 mg/L	EC-PPT (2)	21.33	22.6

**Desorption–Elution and Reuse.** Using Equation (4), we proceeded to establish the yield of these biomasses and determine the new adsorption capacity. Figure 7 shows the adsorption capacities in the different elutions.

The elution processes for each of the treated biomasses using EDTA are observable. *E. crassipes* biomass supports different elutions due to the presence of lignin in its plant structure [40–42]. The addition of PPT resulted in up to 7 times more biomass being recycled. The total biomass sum of EC-PPT (2) was 98 mg/g, which is the highest sum reported for *E. crassipes*. The EC-PPT biomass yielded 62 mg/g, a significant parameter as it has half the concentration of PPT and may be more cost-effective for large-scale use.

**The costs of the treatment systems.** The costs of the treatment systems were determined based on the evaluated biomass, and the unit production costs of 1 kg of material were calculated. The cost of drying, crushing, and logistics to obtain *E. crassipes* biomass is approximately USD 2 per 1 kg [43,44].

The cost of EDTA, which is used in biomasses, is USD 0.5 for about 100 g of the reagent. Sodium tripolyphosphate costs USD 3, and USD 2.5 were spent on 250 mL of it for the EC-PPT biomass, making the total cost USD 5. For the EC-PPT biomass, the cost is USD 8. Acetic acid costs USD 0.5. Table 8 displays the total cost of the two samples.

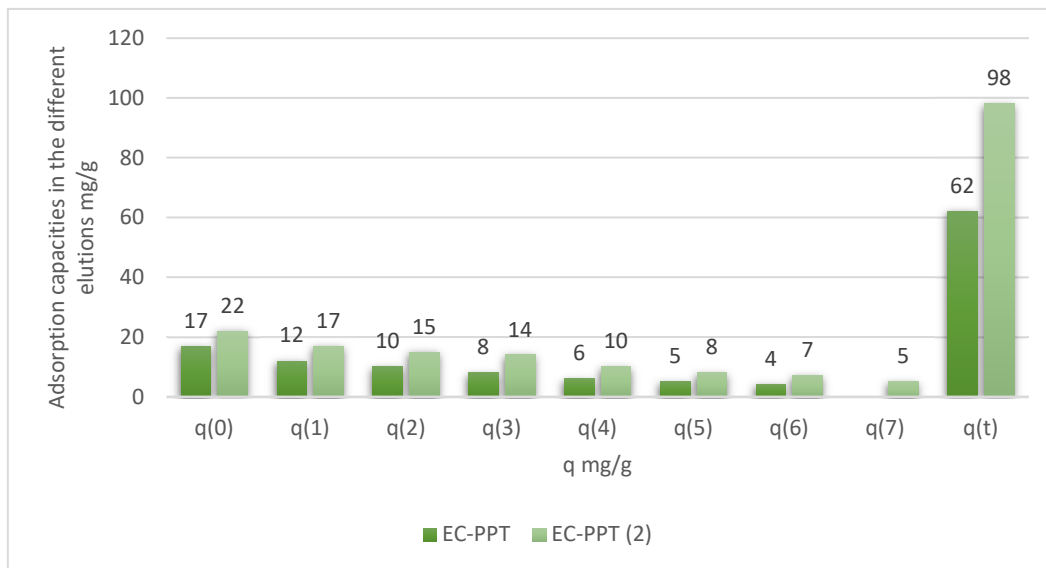


**Figure 7.** Adsorption capacities in the different elutions.

**Table 8.** Costs related to treatment systems.

Cost	EC-PPT (1)	EC-PPT (2)
Capacity total g Cr/100 g material	62	98
Cost (USD) 1 kg material	6.2	8.5
g Cr/(USD)	10	11.5

Table 4 demonstrates the project’s benefit through the adsorption capacity of Cr(VI) and its elutions. The table displays the cost versus adsorption capacity for each biomass, indicating the cost of producing 1 kg of biomass or composite material. Additionally, the yield of adsorption capacity per dollar spent is included.

The EC-PPT biomass (1) has an adsorption capacity indicator of 10 g Cr(VI) per dollar. The second indicator, EC-PPT biomass (2), has an indicator of 11.5 g/USD due to its effectiveness and low cost. However, the EC biomass, despite being the cheapest, has an indicator of only 1.5 g/USD due to its low adsorption capacity compared to other biomasses.

Representative data were obtained using Equation (4) and various bibliographic references to establish a relationship between adsorption capacities and the production cost of 1 kg. It is important to note that associated costs may vary. Table 9 summarizes several biomass treatment processes. The indicator g HV/(USD) shows the amount of heavy metal removed in relation to the adsorption capacity of the biomass, compared to the cost of production/modification of this biomass in US dollars per kg [45].

Unmodified biomasses [1] have a low unit cost, but their g HV/(USD) indicator does not exceed 7.5. However, chemical modifications can significantly improve the adsorption capacity by increasing active sites, as reflected in this indicator [46].

It is worth noting that the investigated adsorption capacities [47–50] for various heavy metals are exceptionally high, surpassing 150 mg/g. The Humulus biomass with EDTA exhibits an impressive adsorption capacity of 398 mg/g. Processing costs for these biomasses should be taken into account, as indicated by the g HV/(USD) which is comparable to that of poorly processed biomasses. By selecting the appropriate biomass and adjusting it to treat the specific heavy metals present in the water, heavy metal adsorption can be optimized.

**Table 9.** Research on the process of elutions.

Reference	Biomass	Recycling	Capacity (mg/g) with the Equation (4)	Cost (USD) 1 kg Material	g HV/(USD)
	EC-PPT (2)	EDTA	98	8.5	11.5
	EC-PPT (1)	EDTA	62	6.2	10
[1]	<i>Crassipes</i>	-	8	3	2.5
[2]	<i>Crassipes</i> + Fe	EDTA	42	3.3	12.7
[2]	<i>crassipes</i>	EDTA	23	3.1	7.4
[20]	Xantate of cellulose	EDTA	51	7	7.2
[20]	Cellulose alkaline	EDTA	32	6	5.3
[46]	<i>Crassipes</i> + EDTA		45	10	4.5
[47]	<i>pinecone shells</i>	HCl	66	10	6.6
[48]	<i>Citrus maxima peel</i>		84	10	8.4
[49]	Kraft pulp/carboxyMethyled	HCl	101	40	2.5
[50]	Chitosan biocomposite	EDTA	146	35	5.3
[51]	<i>Humulus lupulus</i>	EDTA	398	50	7.9
[52]	Lignocellulosic biomass	EDTA	156	10	15.6

#### 4. Conclusions

Two treatment processes have been successfully developed on a pilot scale, providing the necessary parameters to design and develop a treatment system on an industrial scale. The resulting system has a unit cost of approximately USD 8, which is significantly lower than conventional treatment systems in the industrial wastewater treatment sector.

The proposed system has an exceptional capacity to adsorb Cr(VI) and can be reused several times by eluting with EDTA. It is cost-effective and promotes sustainability and compliance with landfill regulations in the tannery sector. This helps to preserve the water resources surrounding these production centers.

The elution processes have been optimized to improve the adsorption of heavy metals, resulting in a production cost of only USD 8.5, with an indicator of 11.5 g HV/(USD). Biomass has a remarkable adsorption capacity of 98 mg/g, making it an extremely effective option for the chemisorption of heavy metals, particularly Cr(VI).

The findings suggest that *E. crassipes* biomass, enhanced with PTT and through EDTA elutions, could be a suitable water remediation technology based on chemisorption technology. This technology could be used for large-scale decontamination of rivers, wetlands, and other water ecosystems contaminated with various heavy metals.

**Author Contributions:** Conceptualization, U.F.C.S. and V.A.B.B.; methodology, U.F.C.S.; software, V.A.B.B.; validation, U.F.C.S.; formal analysis, U.F.C.S. and V.A.B.B.; investigation, U.F.C.S.; resources, V.A.B.B.; data curation, U.F.C.S.; writing—original draft preparation, U.F.C.S.; writing—review and editing, U.F.C.S.; visualization, U.F.C.S. and V.A.B.B.; supervision, U.F.C.S.; project administration, U.F.C.S. and V.A.B.B.; funding acquisition, All authors have read and agreed to the published version of the manuscript.

**Funding:** The “Universidad los Libertadores” funded this research through an internal call.

**Data Availability Statement:** The datasets used and/or analyzed during the current study are available from the corresponding author upon reasonable request.

**Conflicts of Interest:** The author declares no conflicts of interest.

#### References

- Sayago, U.F.C. Design and development of a biotreatment of *E. crassipes* for the decontamination of water with Chromium (VI). *Sci. Rep.* **2021**, *11*, 9326. [[CrossRef](#)] [[PubMed](#)]
- Carreño Sayago, U.F.; Piñeros Castro, Y.; Conde Rivera, L.R. Design of a Fixed-Bed Column with Vegetal Biomass and Its Recycling for Cr(VI) Treatment. *Recycling* **2022**, *7*, 71. [[CrossRef](#)]
- Afroz, S.; Sen, T.K. A review on heavy metal ions and dye adsorption from water by agricultural solid waste adsorbents. *Water Air Soil Pollut.* **2018**, *229*, 225. [[CrossRef](#)]

4. Gradilla-Hernández, M.S.; Díaz-Vázquez, D.; Yebra-Montes, C.; del Castillo, A.F.; Shear, H.; Garcia-Gonzalez, A.; Mazari-Hiriart, M. Assessment of the Potential of Coordinating Two Interacting Monitoring Networks within the Lerma-Santiago Hydrologic System in Mexico. *Water* **2022**, *14*, 1687. [CrossRef]
5. Al-Ghouti, M.A.; Al-Absi, R.S. Mechanistic understanding of the adsorption and thermodynamic aspects of cationic methylene blue dye onto cellulosic olive stones biomass from wastewater. *Sci. Rep.* **2022**, *10*, 15928. [CrossRef]
6. Barquilha, C.E.R.; Cossich, E.S.; Tavares, C.R.G.; Silva, E.A. Biosorption of nickel (II) and copper (II) ions in batch and fixed-bed columns by free and immobilized marine algae *Sargassum* sp. *J. Clean. Prod.* **2017**, *150*, 58–64. [CrossRef]
7. Vinayagam, R.; Dave, N.; Varadavenkatesan, T.; Rajamohan, N.; Sillanpää, M.; Nadda, A.K.; Selvaraj, R. Artificial neural network and statistical modelling of biosorptive removal of hexavalent chromium using macroalgal spent bio-mass. *Chemosphere* **2015**, *296*, 133965. [CrossRef] [PubMed]
8. Ang, T.N.; Young, B.R.; Taylor, M.; Burrell, R.; Aroua, M.K.; Baroutian, S. Breakthrough analysis of continuous fixed-bed adsorption of sevoflurane using activated carbons. *Chemosphere* **2020**, *239*, 124839. [CrossRef] [PubMed]
9. Saade-Cleves, N.; Talero-Munoz, M.D.M.; García-Vargas, D.; Tamayo-Torres, C.S.; Sierra-Pena, J.A.; Torres-Ortiz, M.P.; Palencia-Sánchez, F. The Risk Index Used to Assess the Risk of Heavy Metals, Mainly in Water Sediments, on Human Health in Latin America: A Rapid Review of Literature (December 27, 2022). Available online: <https://ssrn.com/abstract=4313001> (accessed on 13 March 2024). [CrossRef]
10. Ramírez-Canon, A.; Becerra-Quiroz, A.P.; Herrera-Jacquelin, F. Perfluoroalkyl and polyfluoroalkyl substances (PFAS): First survey in water samples from the Bogotá River, Colombia. *Environ. Adv.* **2022**, *8*, 100223. [CrossRef]
11. Hokkanen, S.; Repo, E.; Suopajarvi, T.; Liimatainen, H.; Niinimaa, J.; Sillanpää, M. Adsorption of Ni (II), Cu (II) and Cd (II) from aqueous solutions by amino modified nanostructured microfibrillated cellulose. *Cellulose* **2014**, *21*, 1471–1487. [CrossRef]
12. Lin, S.; Huang, W.; Yang, H.; Sun, S.; Yu, J. Recycling application of waste long-root *Eichhornia crassipes* in the heavy metal removal using oxidized biochar derived as adsorbents. *Bioresour. Technol.* **2020**, *314*, 123749. [CrossRef] [PubMed]
13. Ajitha, P.; Vijayalakshmi, K.; Saranya, M.; Gomathi, T.; Rani, K.; Sudha, P.N.; Sukumaran, A. Removal of toxic heavy metal lead (II) using chitosan oligosaccharide-graft-maleic anhydride/polyvinyl alcohol/silk fibroin composite. *Int. J. Biol. Macromol.* **2017**, *104*, 1469–1482.
14. Hokkanen, S.; Repo, E.; Westholm, L.J.; Lou, S.; Sainio, T.; Sillanpää, M. Adsorption of Ni<sup>2+</sup>, Cd<sup>2+</sup>, PO<sub>4</sub><sup>3-</sup> and NO<sub>3</sub><sup>-</sup> from aqueous solutions by nanostructured microfibrillated cellulose modified with carbonated hydroxyapatite. *Chem. Eng. J.* **2014**, *252*, 64–74. [CrossRef]
15. Sahota, S.; Pande, K.M.; Suresh, S.; Arisutha, S.; Singh, D.; Shah, G. Biological Pretreatment of Water Hyacinth (*Eichhornia crassipes*) for Biofuel Production-A Review. *J. Biofuels Bioenergy* **2016**, *2*, 97–101. [CrossRef]
16. Wu, S.; Kan, J.; Dai, X.; Shen, X.; Zhang, K.; Zhu, M. Ternary carboxymethyl chitosan-hemicellulose-nanosized TiO<sub>2</sub> composite as effective adsorbent for removal of heavy metal contaminants from water. *Fibers Polym.* **2017**, *18*, 22–32. [CrossRef]
17. Hokkanen, S.; Bhatnagar, A.; Repo, E.; Lou, S.; Sillanpää, M. Calcium hydroxyapatite microfibrillated cellulose composite as a potential adsorbent for the removal of Cr(VI) from aqueous solution. *Chem. Eng. J.* **2016**, *283*, 445–452. [CrossRef]
18. Lin, S.; Yang, H.; Na, Z.; Lin, K. A novel biodegradable arsenic adsorbent by immobilization of iron oxyhydroxide (FeOOH) on the root powder of long-root *Eichhornia crassipes*. *Chemosphere* **2018**, *192*, 258–266. [CrossRef] [PubMed]
19. Carreño Sayago, U.F. Design, Scaling, and Development of Biofilters with *E. crassipes* for Treatment of Water Contaminated with Cr(VI). *Water* **2021**, *13*, 1317. [CrossRef]
20. Sayago, U.F.C.; Ballesteros Ballesteros, V. Development of a treith Cr(VI) using cellulose xanthogenate from *E. crassipes* on a pilot scale. *Sci. Rep.* **2023**, *13*, 1970. [CrossRef] [PubMed]
21. Tan, L.; Zhu, D.; Zhou, W.; Mi, W.; Ma, L.; He, W. Preferring cellulose of *Eichhornia crassipes* to prepare xanthogenate to other plant materials and its adsorption properties on copper. *Bioresour. Technol.* **2008**, *99*, 4460–4466. [CrossRef] [PubMed]
22. Widiyowati, I.I.; Nurhadi, M.; Hatami, M.; Yuan, L.S. Effective TiO<sub>2</sub>-Sulfonated Carbon-derived from *Eichhornia crassipes* in The Removal of Methylene Blue and Congo Red Dyes from Aqueous Solution. *Bull. Chem. React. Eng. Catal.* **2020**, *15*, 476–489. [CrossRef]
23. Sayago, U.F.C. Diseño y evaluación de un biosistema de tratamiento a escala piloto de aguas de curtiembres a través de la *Eichhornia crassipes*. *Rev. Colomb. Biotecnol.* **2016**, *18*, 74–81. [CrossRef]
24. Sharma, K.; Singh, N.; Sharma, R. *Eichhornia crassipes* leaves biomass harvested from heavy metal contaminated water for biodiesel production potential. *Res. Crops* **2021**, *22*, 720–726.
25. Hua, M.; Zhang, S.; Pan, B.; Zhang, W.; Lv, L.; Zhang, Q. Heavy metal removal from water/wastewater by nanosized metal oxides: A review. *J. Hazard. Mater.* **2021**, *211*, 317–331. [CrossRef] [PubMed]
26. Wang, C.; Zhan, Y.; Wu, Y.; Shi, X.; Du, Y.; Luo, Y.; Deng, H. TiO<sub>2</sub>/rectorite-trapped cellulose composite nanofibrous mats for multiple heavy metal adsorption. *Int. J. Biol. Macromol.* **2020**, *183*, 245–253. [CrossRef] [PubMed]
27. Ajmani, A.; Patra, C.; Subbiah, S.; Narayanasamy, S. Packed bed column studies of hexavalent chromium adsorption by zinc chloride activated carbon synthesized from *Phanera vahlii* fruit biomass. *J. Environ. Chem. Eng.* **2020**, *8*, 103825. [CrossRef]
28. Mahmoud, A.E.D.; Fawzy, M.; Hosny, G.; Obaid, A. Equilibrium, kinetic, and diffusion models of chromium (VI) removal using *Phragmites australis* and *Ziziphus spina-christi* biomass. *Int. J. Environ. Sci. Technol.* **2021**, *18*, 2125–2136. [CrossRef]
29. Vijayalakshmi, K.; Gomathi, T.; Latha, S.; Hajeeth, T.; Sudha, P.N. Removal of copper (II) from aqueous solution using nanochitosan/sodium alginate/microcrystalline cellulose beads. *Int. J. Biol. Macromol.* **2016**, *82*, 440–452. [CrossRef]

30. Carreño-Sayago, U.F. Development of microspheres using water hyacinth (*Eichhornia crassipes*) for treatment of contaminated water with Cr(VI). *Environ. Dev. Sustain.* **2021**, *23*, 4735–4746. [[CrossRef](#)]
31. Wang, J.; Liu, H.; Yang, S.; Zhang, J.; Zhang, C.; Wu, H. Physicochemical characteristics and sorption capacities of heavy metal ions of activated carbons derived by activation with different alkyl phosphate triesters. *Appl. Surf. Sci.* **2014**, *316*, 443–450. [[CrossRef](#)]
32. Ammar, N.S.; Elhaes, H.; Ibrahim, H.S.; Ibrahim, M.A. A novel structure for removal of pollutants from wastewater. *Spectrochim. Acta Part A Mol. Biomol. Spectrosc.* **2014**, *121*, 216–223. [[CrossRef](#)]
33. da Cunha, L.P.; Casciatori, F.P.; Vicente, I.V.; Garcia, R.L.; Thoméo, J.C. Metarhizium anisopliae conidia production in packed-bed bioreactor using rice as substrate in successive cultivations. *Process Biochem.* **2020**, *97*, 104–111. [[CrossRef](#)]
34. Tikhomirova, T.S.; But, S.Y. Laboratory scale bioreactor designs in the processes of methane bioconversion: Mini-review. *Biotechnol. Adv.* **2021**, *47*, 107709. [[CrossRef](#)] [[PubMed](#)]
35. Bringas, A.; Bringas, E.; Ibañez, R.; San-Román, M.F. Fixed-bed columns mathematical modeling for selective nickel and copper recovery from industrial spent acids by chelating resins. *Sep. Purif. Technol.* **2023**, *313*, 123457. [[CrossRef](#)]
36. Dawodu, F.A.; Akpan, B.M.; Akpomie, K.G. Sequestered capture and desorption of hexavalent chromium from solution and textile wastewater onto low cost Heinsia crinita seed coat biomass. *Appl. Water Sci.* **2024**, *10*, 1–15. [[CrossRef](#)]
37. Tallman, P.S.; Collins, S.; Salmon-Mulanovich, G.; Rusyidi, B.; Kothadia, A.; Cole, S. Water insecurity and gender-based violence: A global review of the evidence. *Wiley Interdiscip. Rev. Water* **2023**, *10*, e1619. [[CrossRef](#)]
38. Souza Veloso, D.E.; Werderits Silva, D.E.; de Andrade Aguiar, L.G.; Abrãao, R.; de Souza Sampaio, N.A. Application of the exponential distribution to improve environmental quality in a company in the south of Rio de Janeiro State. *GeSec Rev. Gest. E Secr.* **2023**, *14*, 15695–15704. [[CrossRef](#)]
39. Lesmana, S.O.; Febriana, N.; Soetaredjo, F.E.; Sunarso, J.; Ismadji, S. Studies on potential applications of biomass for the separation of heavy metals from water and wastewater. *Biochem. Eng. J.* **2009**, *44*, 19–41. [[CrossRef](#)]
40. Fan, H.; Chen, S.; Li, Z.; Liu, P.; Xu, C.; Yang, X. Assessment of heavy metals in water, sediment and shellfish organisms in typical areas of the Yangtze River Estuary, China. *Mar. Pollut. Bull.* **2020**, *151*, 110864. [[CrossRef](#)] [[PubMed](#)]
41. Chatterjee, A.; Abraham, J. Desorption of heavy metals from metal loaded sorbents and e-wastes: A review. *Biotechnol. Lett.* **2019**, *41*, 319–333. [[CrossRef](#)]
42. Jiang, X.; An, Q.D.; Xiao, Z.Y.; Zhai, S.R.; Shi, Z. Versatile core/shell-like alginate@polyethylenimine composites for efficient removal of multiple heavy metal ions ( $Pb^{2+}$ ,  $Cu^{2+}$ ,  $CrO_4^{2-}$ ): Batch and fixed-bed studies. *Mater. Res. Bull.* **2019**, *118*, 110526. [[CrossRef](#)]
43. Júnior, W.N.; Silva, M.G.C.; Vieira, M.G.A. Competitive fixed-bed biosorption of Ag (I) and Cu (II) ions on Sargassum filipendula seaweed waste. *J. Water Process Eng.* **2020**, *36*, 101294. [[CrossRef](#)]
44. Sayago, U.F.C.; Castro, Y.P.; Rivera, L.R.C.; Mariaca, A.G. Estimation of equilibrium times and maximum capacity of adsorption of heavy metals by *E. crassipes*. *Environ. Monit. Assess.* **2020**, *192*, 141. [[CrossRef](#)] [[PubMed](#)]
45. Sayago, U.F.C.; Ballesteros Ballesteros, V. Recent Advances in the Treatment of Industrial Wastewater from Different Celluloses in Continuous Systems. *Polymers* **2023**, *15*, 3996. [[CrossRef](#)] [[PubMed](#)]
46. Sayago, U.F.C. Design and Development of a Pilot-Scale Industrial Wastewater Treatment System with Plant Biomass and EDTA. *Water* **2023**, *15*, 3484. [[CrossRef](#)]
47. Amar, M.B.; Mallek, M.; Valverde, A.; Monclús, H.; Myers, T.G.; Salvadó, V.; Cabrera-Codony, A. Competitive heavy metal adsorption on pinecone shells: Mathematical modelling of fixed-bed column and surface interaction insights. *Sci. Total Environ.* **2024**, *917*, 170398. [[CrossRef](#)] [[PubMed](#)]
48. Chao, H.P.; Chang, C.C.; Nieva, A. Biosorption of heavy metals on Citrus maxima peel, passion fruit shell, and sugarcane bagasse in a fixed-bed column. *J. Ind. Eng. Chem.* **2014**, *20*, 3408–3414. [[CrossRef](#)]
49. Islam, M.S.; Rahaman, M.S.; Barbeau, B. Removal of Pb (II), Zn (II), Cu (II), and As (III) ions from water using kraft pulp-based carboxymethylated cellulose in a fixed-bed column adsorption process. *J. Environ. Chem. Eng.* **2023**, *11*, 111181. [[CrossRef](#)]
50. Solgi, M.; Mohamed, M.H.; Udoetok, I.A.; Steiger, B.G.; Wilson, L.D. Evaluation of a granular Cu-modified chitosan biocomposite for sustainable sulfate removal from aqueous media: A batch and fixed-bed column study. *Int. J. Biol. Macromol.* **2024**, 129275.
51. Perendija, J.; Ljubić, V.; Popović, M.; Milošević, D.; Arsenijević, Z.; Đuriš, M.; Cvetković, S. Assessment of waste hop (*Humulus Lupulus*) stems as a biosorbent for the removal of malachite green, methylene blue, and crystal violet from aqueous solution in batch and fixed-bed column systems: Biosorption process and mechanism. *J. Mol. Liq.* **2024**, *394*, 123770. [[CrossRef](#)]
52. Safardastgerdi, M.; Ardejani, F.D.; Mahmoodi, N.M. Lignocellulosic biomass functionalized with EDTA dianhydride for removing Cu (II) and dye from wastewater: Batch and fixed-bed column adsorption. *Miner. Eng.* **2023**, *204*, 108423. [[CrossRef](#)]

**Disclaimer/Publisher's Note:** The statements, opinions and data contained in all publications are solely those of the individual author(s) and contributor(s) and not of MDPI and/or the editor(s). MDPI and/or the editor(s) disclaim responsibility for any injury to people or property resulting from any ideas, methods, instructions or products referred to in the content.